Structure-guided development of deoxycytidine kinase inhibitors with nanomolar affinity and improved metabolic stability

Julian Nomme[1,#, §, †], Zheng Li[3,4, #], Raymond M. Gipson[3,4, #], Jue Wang[3,4, #], Amanda L. Armijo[3,4], Thuc Le[3,4], Soumya Poddar[3,4], Tony Smith[3,4], Bernard D. Santarsiero[2], Hien-Anh Nguyen[1], Johannes Czernin[3,4], Anastassia N. Alexandrova[6], Michael E. Jung[6], Caius C. Radu[3,4] and Arnon Lavie[1*]

Supplementary Scheme 1. Synthesis route for racemic methyl linker compound 9.

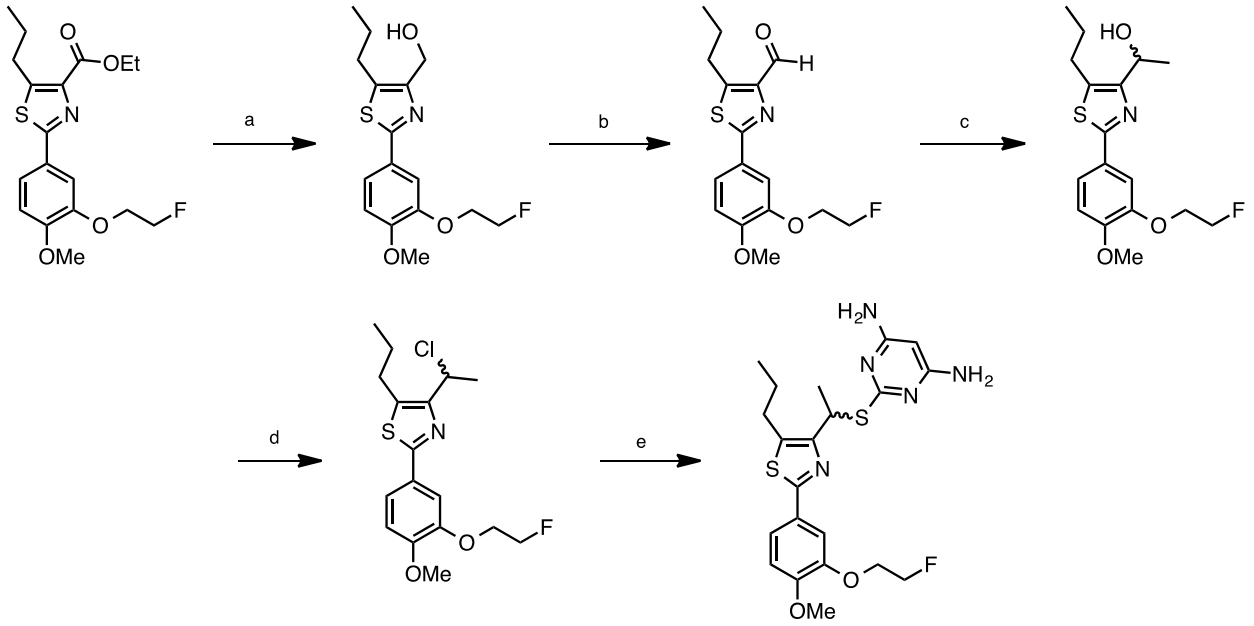

Reagents and conditions: (a) Diisobutylaluminium hydride, tetrahydrofuran, (previous work); (b) Dess–Martin periodinane, dichloromethane, 23 °C, 80%; (c) Methylmagnesium iodide, tetrahydrofuran, 0 °C, 86%; (d) Thionyl chloride, dichloromethane, 23 °C, 96%; (e) 4,6-diamino-2-mercaptopyrimidine, potassium carbonate, DMF, 80 °C, 66%.

Supplementary Scheme 2. Synthesis route for racemic methyl linker compound 10

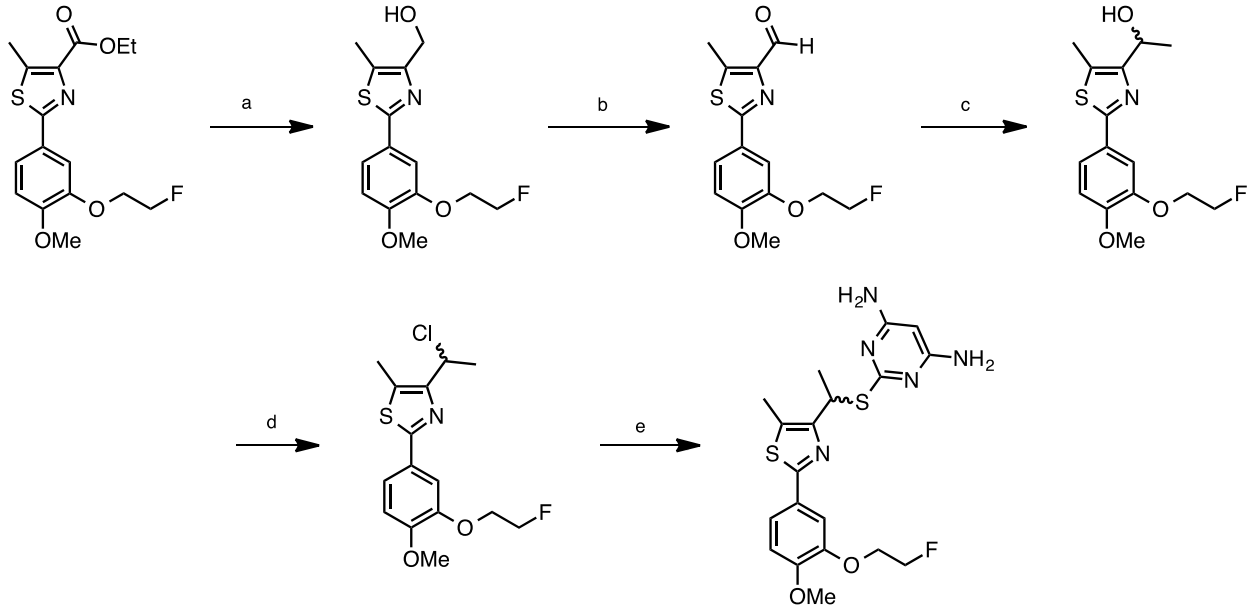

Reagents and conditions: (a) Diisobutylaluminium hydride, tetrahydrofuran, (previous work); (b) Dess–Martin periodinane, dichloromethane, 23 °C, 70%; (c) Methylmagnesium iodide, tetrahydrofuran, 0 °C, 68%; (d) Thionyl chloride, dichloromethane, 23 °C, 94%; (e) 4,6-diamino-2-mercaptopyrimidine, potassium carbonate, DMF, 80 °C, 64%.

SUPPLEMENTARY FIGURE S1.

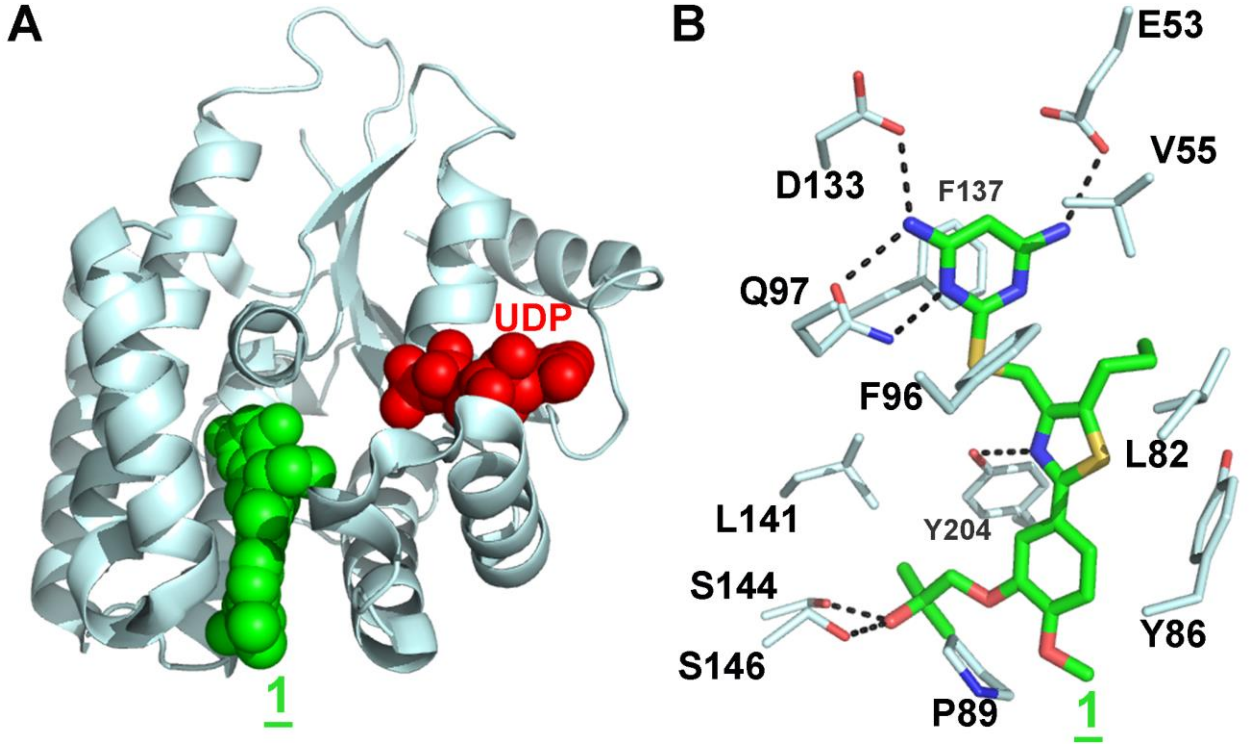

Binding of **1** to human dCK. A) Ribbon diagram of a dCK monomer (light blue) with the observed molecule of **1** bound (green spheres) at the active site (PDB ID 4L5B). The nucleotide UDP (red) was also present in the complex. B) The interactions between **1** and dCK. dCK residues contributing to the interaction with **1** (green sticks) are represented as light blue sticks. Polar interactions are indicated as broken black lines.

SUPPLEMENTARY FIGURE S2

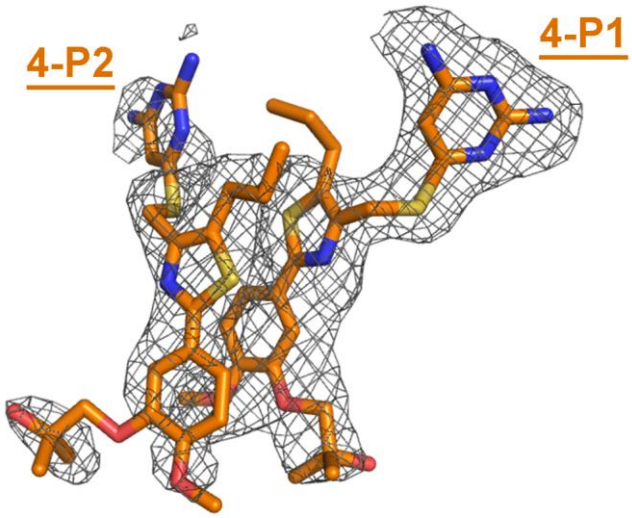

Fo-Fc map contoured at 3 sigma around compound **4** from protomer A. Compound **4** was removed from the model that then underwent several rounds of refinement to eliminate model bias. This inhibitor binds as two molecules at the active site of dCK at Position-1 and -2 and labeled **4-P1** and **4-P2** respectively (PDB ID 4Q18).

SUPPLEMENTARY FIGURE S3

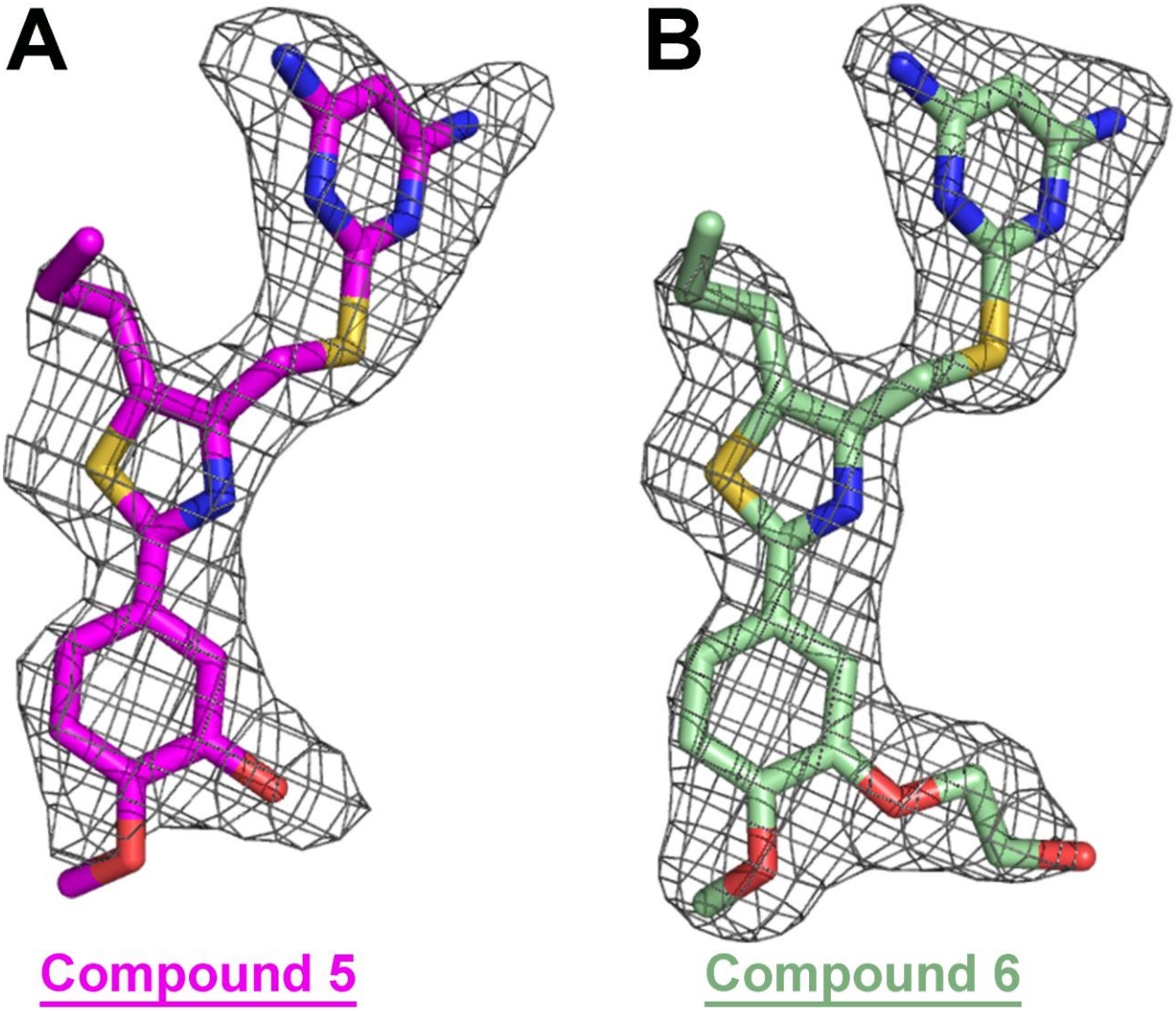

Fo-Fc map contoured at 2.5 sigma around compounds **5** and **6** from protomer A. A) Compound **5** was removed from the model that then underwent several rounds of refinement to eliminate model bias (PDB ID 4Q19). B) Same for compound **6** (PDB ID 4Q1A).

SUPPLEMENTARY FIGURE S4

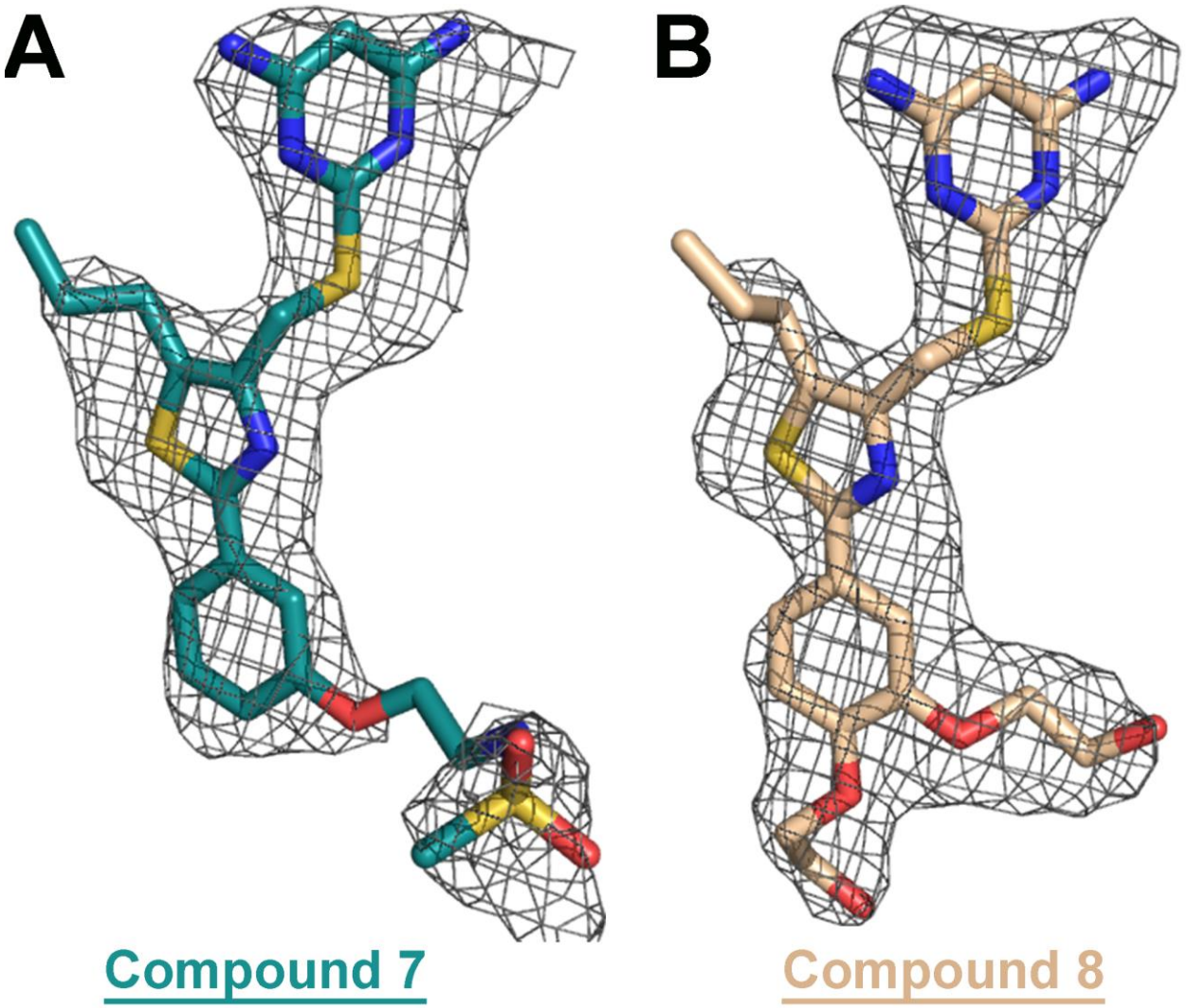

Fo-Fc map contoured at 2.0 sigma around compounds **7** and **8** from protomer A. A) Compound **7** was removed from the model that then underwent several rounds of refinement to eliminate model bias (PDB ID 4Q1B). B) Same for compound **8** (PDB ID 4Q1C).

SUPPLEMENTARY FIGURE S5

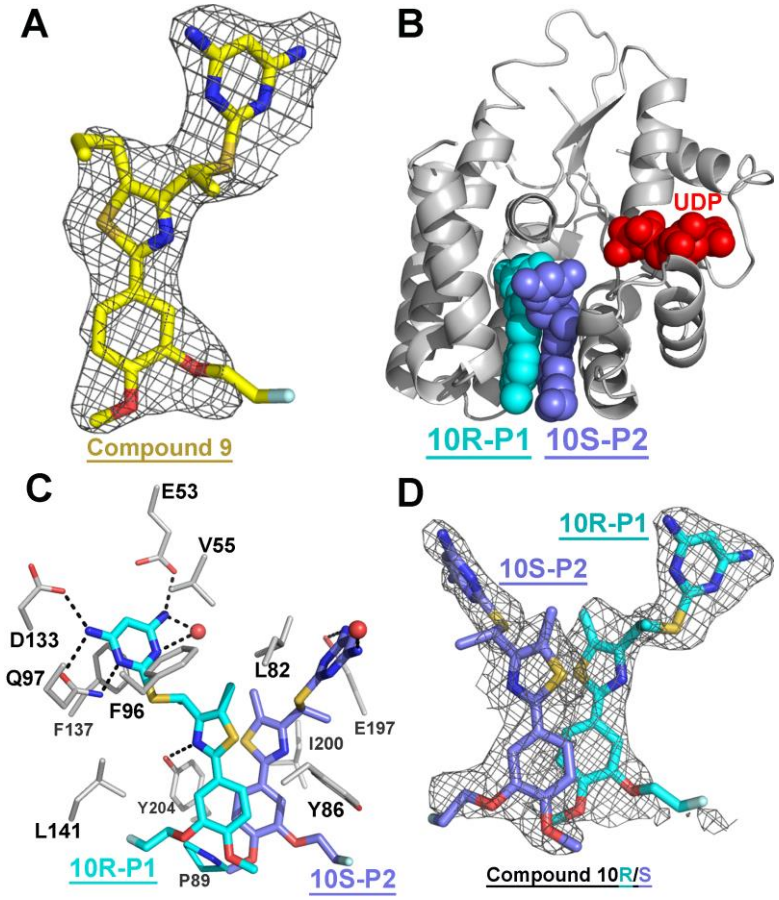

Fo-Fc map contoured at 2.0 sigma around compounds **9** and **10** from protomer A and binding of **10** to human dCK. A) Compound **9** was removed from the model that then underwent several rounds of refinement to eliminate model bias (PDB ID 4Q1D). B) Ribbon diagram of a dCK monomer (light gray) with the observed molecules of **10** bound at the active site (cyan and plum spheres). This inhibitor binds two molecules at the active site of dCK. Due to the presence of a chiral carbon within the linker and the use of a racemic mixture, we observe the R enantiomer binding at Position-1 (**10R-P1** in cyan) and the S enantiomer binding at Position-2 (**10S-P2** in plum), (PDB ID 4Q1E). The nucleotide UDP (red) was also present in the complex. C) The interactions between **10-R and -S** and dCK. dCK residues contributing to the interaction with **10** (10-R and 10-S as cyan and plum sticks respectively) are represented as light gray sticks. Polar interactions are indicated as broken black lines. D) Same as A) for compound **10**.

SUPPLEMENTARY FIGURE S6

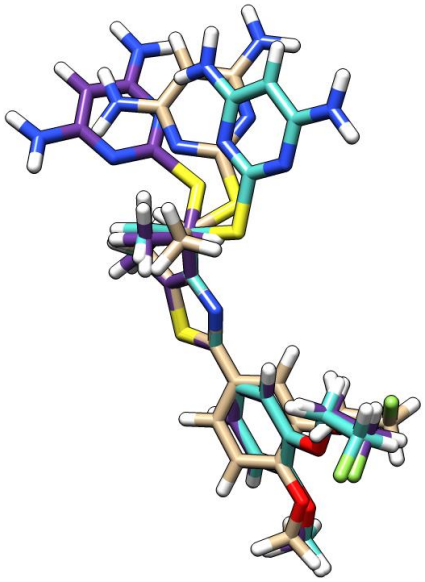

Relative orientation of **10R** (cyan) and **10S** (plum) optimized in solution, compared to the pose of **10R** bound at Position 1 in crystal structure (tan). The structures are aligned according to the thiazole rings. This illustrates the conformational change that must occur for the molecule to move out of solution and bind with the protein. Both **10R** and **10S** incur an energy penalty in undergoing this conformational change, but the penalty for **10R** is much less than the penalty for **10S**.

Table S1. In vitro biological data in CEM cells for compounds 1-12 and S1-S31[a,b]

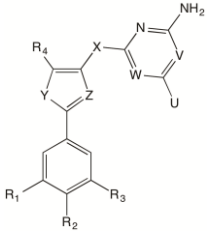

Compound	R_1	R_2	R_3	R_4	U	V	W	Y	Z	X	IC_{50} (nM)
1	H	OCH_3	$OCH_2C(CH_3)_2OH$	$CH_2CH_2CH_3$	NH_2	C	N	S	N	CH_2S	1.4
2	H	OCH_3	$OCH_2CH_2NHSO_2Me$	$CH_2CH_2CH_3$	NH_2	C	N	S	N	CH_2S	4.9
3	H	OCH_3	$OCH_2C(CH_3)_2OH$	$CH_2CH_2CH_3$	H	C	N	S	N	CH_2S	21.8
4	H	OCH_3	$OCH_2C(CH_3)_2OH$	$CH_2CH_2CH_3$	NH_2	N	C	S	N	CH_2S	395 (±14.2)
5	H	OCH_3	OH	$CH_2CH_2CH_3$	NH_2	C	N	S	N	CH_2S	18.6
6	H	OCH_3	OCH_2CH_2OH	$CH_2CH_2CH_3$	NH_2	C	N	S	N	CH_2S	1.15
7	H	H	$OCH_2CH_2NHSO_2Me$	$CH_2CH_2CH_3$	NH_2	C	N	S	N	CH_2S	11.6
8	H	$O(CH_2)_2OH$	OCH_2CH_2OH	$CH_2CH_2CH_3$	NH_2	C	N	S	N	CH_2S	0.9
9	H	OCH_3	OCH_2CH_2F	$CH_2CH_2CH_3$	NH_2	C	N	S	N	$CH(CH_3)S$	10.0
10	H	OCH_3	OCH_2CH_2F	CH_3	NH_2	C	N	S	N	$CH(CH_3)S$	7.0
11 R	H	Note[c]	OCH_2CH_3	CH_3	NH_2	C	N	S	N	$CH(CH_3)S$	1.25
11 S	H	Note[c]	OCH_2CH_3	CH_3	NH_2	C	N	S	N	$CH(CH_3)S$	429.5 (±34.1)
12 R	H	OCH_3	$OCH_2CH_2NHSO_2Me$	CH_3	NH_2	C	N	S	N	$CH(CH_3)S$	3.7 (±0.8)
12 S	H	OCH_3	$OCH_2CH_2NHSO_2Me$	CH_3	NH_2	C	N	S	N	$CH(CH_3)S$	94.0 (±14.4)
S1 DI-47	H	OCH_3	$OCH_2C(CH_3)_2OH$	$CH_2CH_2CH_3$	NH_2	C	N	S	N	CD_2S	4.0 (±2.2)

S2 DI-50	H	Note[d]	$OCH_2CH_2NHSO_2Me$	$CH_2CH_2CH_3$	NH_2	C	N	S	N	CH_2S	1,200(±312)
S3 DI-51	H	OCH_3	$OCH_2CH_2CH_2F$	$CH_2CH_2CH_3$	NH_2	C	N	S	N	CH_2S	2.5 (±0.35)
S4 DI-52	H	OCH_2CH_2F	OCH_2CH_3	$CH_2CH_2CH_3$	NH_2	C	N	S	N	CH_2S	2.8 (±1.6)
S5 DI-53	H	F	$OCH_2CH_2CH_2F$	$CH_2CH_2CH_3$	NH_2	C	N	S	N	CH_2S	31.7(±11.9)
S6 DI-54	H	F	OCH_2CH_2F	$CH_2CH_2CH_3$	NH_2	C	N	S	N	CH_2S	23.3 (±13)
S7 DI-55	H	N/A[e]	OCH_2CH_2F	$CH_2CH_2CH_3$	NH_2	C	N	S	N	CH_2S	6.8 (±1.7)
S8 DI-56	H	N/A[e]	OCH_2CH_2F	$CH_2CH_2CH_3$	NH_2	C	N	S	N	CD_2S	30 (±4)
S9 DI-57	H	OCH_3	OCH_2CH_2F	$CH_2CH_2CH_3$	NH_2	C	N	S	N	CD_2S	3.1 (±1.1)
S10 DI-58	H	OCH_3	$O(CH_2)_2O(CH_2)_2O(CH_2)_2X$[f]	$CH_2CH_2CH_3$	NH_2	C	N	S	N	CH_2S	4.7 (±1.6)
S11 DI-59	H	OCH_3	$O(CH_2)_2O(CH_2)_2O(CH_2)_2OH$	$CH_2CH_2CH_3$	NH_2	C	N	S	N	CH_2S	1.06 (±0.15)
S12 DI-60	H	OCH_3	OCH_2CH_2F	CH_3	NH_2	C	N	O	C	CH_2S	13,840(±280)
S13 DI-61	H	OCH_3	$OCH_2CH_2NHSO_2Me$	$CH_2CH_2CH_3$	NH_2	C	N	S	N	CD_2S	3.04 (±0.704)
S14 DI-62	H	OCH_2CH_2F	OCH_3	CH_3	NH_2	C	N	O	C	CH_2S	276 (±179)
S15 DI-64	H	OCH_3	OCH_2CH_2F	$CH_2CH_2CH_3$	NH_2	C	N	S	N	CH_2CH_2	664 (±360)
S16 DI-65	H	OCH_3	$O(CH_2)_2O(CH_2)_2O(CH_2)_2F$	$CH_2CH_2CH_3$	NH_2	C	N	S	N	CH_2S	4.22 (±1.98)
S17 DI-66	H	H	$O(CH_2)_2O(CH_2)_2O(CH_2)_2F$	$CH_2CH_2CH_3$	NH_2	C	N	S	N	CH_2S	69.08 (±46.41)
S18 DI-67	H	OCH_2CH_2F	OCH_3	CH_3	NH_2	C	N	S	C	CH_2S	262 (±150)
S19 DI-69	F	H	$O(CH_2)_2O(CH_2)_2O(CH_2)_2F$	$CH_2CH_2CH_3$	NH_2	C	N	S	N	CH_2S	33.68 (±3.59)
S20 DI-70	H	OCH_3	$O(CH_2)_2O(CH_2)_2O(CH_2)_2OCH_3$	$CH_2CH_2CH_3$	NH_2	C	N	S	N	CH_2S	3.31 (±0.44)
S21 DI-71	H	Note[c]	OCH_2CH_3	$CH_2CH_2CH_3$	NH_2	C	N	S	N	CH_2S	2.37 (±0.44)
S22 DI-73	H	OCH_3	$O(CH_2)_2O(CH_2)_2O(CH_2)_2OCH_3$	$CH_2CH_2CH_3$	NH_2	C	N	S	N	$CH(CH_3)S$	6.0 (±2.4)

S23 DI-74	H	OCH_3	$O(CH_2)_2O(CH_2)_2O(CH_2)_2OCH_3$	CH_3	NH_2	C	N	S	N	$CH(CH_3)S$	8.03 (±3.16)
S24 DI-76	H	Note[c]	OCH_3	CH_3	NH_2	C	N	S	N	$CH(CH_3)S$	6.1 (±3.2)
S25 DI-77	H	OCH_3	$O(CH_2)_2O(CH_2)_2O(CH_2)_2OCH_3$	Cpr[g]	NH_2	C	N	S	N	CH_2S	23 (±20)
S26 DI-79	H	OCH_3	$O(CH_2)_2O(CH_2)_2O(CH_2)_2OCH_3$	CH_3	NH_2	C	N	S	N	CH_2S	9.1 (n=1)
S27 DI-80	H	OCH_3	$O(CH_2)_2O(CH_2)_2O(CH_2)_2OCH_3$	Cpr[g]	NH_2	C	N	S	N	$CH(CH_3)S$	3.7 (n=1)
S28 DI-81	H	OCH_3	$O(CH_2)_2O(CH_2)_2O(CH_2)_2OCH_3$	Phenyl	NH_2	C	N	S	N	$CH(CH_3)S$	98.9 (n=1)
S29 DI-83	H	Note[h]	$O(CH_2)_2O(CH_2)_2O(CH_2)_2OCH_3$	CH_3	NH_2	C	N	S	N	$CH(CH_3)S$	61.4 (n=1)
S30 DI-84	H	Note[h]	$OCH_2CH_2NHSO_2Me$	CH_3	NH_2	C	N	S	N	$CH(CH_3)S$	200.3(n=1)
S31 DI-85	F	H	$OCH_2CH_2NHSO_2Me$	CH_3	NH_2	C	N	S	N	$CH(CH_3)S$	9.07 (±2.24)

[a]IC50 values based on inhibition of 3H-deoxycytidine (dCyd) uptake in CEM cells. Values reported are the mean ± SD of at least n = 2 independent experiments. [b]Value reported for n = 1. [c]$R_2=O(CH_2)_2O(CH_2)_2O(CH_2)_2OCH_3$. [d]$R_2=N(SO_2Me)(CH_2CH_2NHSO_2Me)$. [e]2,4-disubstituted pyridine ring. [f]3,5-diaminopyrimidine thiol. [g]Cpr=cyclopropyl. [h]$R_2=OCH_2CH_2NHSO_2Me$.

Supplementary Spectra for Compounds 3, 4, 9, 10, 11R, 11S, and 12S

1-(5-(4-(((4-aminopyrimidin-2-yl)thio)methyl)-5-propylthiazol-2-yl)-2-methoxyphenoxy)-2-methylpropan-2-ol (3 = DI-48). ^{1}H NMR (500 MHz, Acetone-d_6) δ 7.99 (d, J = 6.0 Hz, 1H), 7.53 (d, J = 2.0 Hz, 1H), 7.45 (dd, J = 8.5, 2.0 Hz, 1H), 7.03 (d, J = 8.5 Hz, 1H), 6.31 (br s, 2H), 6.28 (d, J = 5.5 Hz, 1H), 4.48 (s, 2H), 3.88 (s, 3H), 3.88 (s, 2H), 2.93 (t, J = 7.5 Hz, 2H), 1.73 – 1.64 (m, 2H), 1.32 (s, 6H), 0.99 (t, J = 7.0 Hz, 3H); ^{13}C NMR (125 MHz, Acetone-d_6) δ 170.4, 163.8, 163.5, 155.3, 151.5, 149.3, 148.4, 134.7, 126.9, 119.4, 112.2, 111.3, 101.0, 77.7, 69.2, 55.5, 28.3, 28.1, 26.0 (2), 25.2, 13.1; HRMS-ESI (*m/z*) $[M + H]^+$ calcd for $C_{22}H_{28}N_4O_3S_2$ H, 461.1681; found 461.1667.

1-(5-(4-(((2,6-diaminopyrimidin-4-yl)thio)methyl)-5-propylthiazol-2-yl)-2-methoxyphenoxy)-2-methylpropan-2-ol (4 = DI-49) ^{1}H NMR (500 MHz, $CDCl_3$) δ 7.40 – 7.35 (m, 2H), 7.04 (d, J = 8.5 Hz, 1H), 6.21 (s, 2H), 5.99 (s, 2H), 5.67 (s, 1H), 4.60 (s, 1H), 4.39 (s, 2H), 3.82 (s, 3H), 3.76 (s, 2H), 2.83 (t, J = 7.5 Hz, 2H), 1.60 – 1.52 (m, 2H), 1.22 (s, 6H), 0.92 (t, J = 7.0 Hz, 3H); ^{13}C NMR (125 MHz, DMSO-d_6) δ 163.8, 163.4, 162.4, 150.8, 148.7, 148.1, 134.8, 126.0, 119.2, 112.4, 110.3, 90.2, 77.0, 68.8, 55.9, 54.9, 27.7, 26.7 (2), 26.1, 24.9, 13.5; HRMS-ESI (*m/z*) $[M + H]^+$ calcd for $C_{22}H_{29}N_5O_3S_2$ H, 476.1790; found 476.1798.

2-((1-(2-(3-(2-fluoroethoxy)-4-methoxyphenyl)-5-propylthiazol-4-yl)ethyl)thio)pyrimidine-4,6-diamine (9 = DI-68). ^{1}H NMR (500 MHz, $CDCl_3$) δ 7.55 (d, J = 2.0 Hz, 1H), 7.44 (dd, J = 8.5, 2.0 Hz, 1H), 6.88 (d, J = 8.5 Hz, 1H), 5.25 (s, 1H), 5.24 (q, J = 7.0 Hz, 1H), 4.87 (dd, J = 5.6, 2.8 Hz, 1H), 4.77 (dd, J =5.6, 2.8 Hz, 1H), 4.55 (s, 4H), 4.47 (dd, J = 5.0, 3.5 Hz, 1H), 4.34 (dd, J = 5.0, 3.5 Hz, 1H), 3.90 (s, 3H), 2.98 – 2.79 (m, 2H), 1.81 (d, J = 7.0 Hz, 3H), 1.75 – 1.58 (m, 2H), 1.00 (t, J = 7.0 Hz, 3H); ^{13}C NMR (125 MHz, $CDCl_3$) δ 170.8, 163.8, 163.2 (2), 153.0, 150.9, 148.0, 133.0, 127.4, 120.3, 111.7, 111.6, 81.9 (d, J_{CF} = 170.6 Hz), 80.6, 68.4 (d, J_{CF} = 20.6 Hz), 56.1, 37.8, 28.5, 25.3, 22.4, 13.9; HRMS-ESI (*m/z*) $[M + H]^+$ calcd for $C_{21}H_{26}FN_5O_2S_2$ H, 464.1590; found 464.1567.

2-((1-(2-(3-(2-fluoroethoxy)-4-methoxyphenyl)-5-methylthiazol-4-yl)ethyl)thio)pyrimidine-4,6-diamine (10 = DI-72). ^{1}H NMR (500 MHz, CD_3OD) δ 7.53 (s, 1H), 7.43 (d, J = 8.4 Hz, 1H), 7.02 (d, J = 8.4 Hz, 1H), 5.34 – 5.30 (m, 2H), 4.82 – 4.80 (m, 1H), 4.72 – 4.70 (m, 1H), 4.35 – 4.34 (m, 1H), 4.30 – 4.28 (m, 1H), 2.52 (s, 3H), 1.75 (d, J = 7.0 Hz, 3H); ^{13}C NMR (125 MHz, CD_3OD) δ 170.4, 165.8, 165.2, 154.8, 152.7, 149.7, 128.6, 128.1, 121.5, 113.3, 112.8, 83.8, 82.5, 80.6, 70.1, 70.0, 56.5, 38.4, 22.20, 11.5; HRMS-ESI (*m/z*) $[M+H]^+$ calcd for $C_{19}H_{22}FN_5O_2S_2$ H, 436.1277; found 436.1270.

(*R*)-2-((1-(2-(3-Ethoxy-4-(2-(2-(2-methoxyethoxy)ethoxy)ethoxy)phenyl)-5-methylthiazol-4-yl)ethyl)thio)pyrimidine-4,6-diamine (11R = R-DI-75).
$[\alpha]^{21}_D$ = +265.7 (*c* = 0.22 acetone) (ee = 99%).

(*S*)-2-((1-(2-(3-Ethoxy-4-(2-(2-(2-methoxyethoxy)ethoxy)ethoxy)phenyl)-5-methylthiazol-4-yl)ethyl)thio)pyrimidine-4,6-diamine (11S = S-DI-75).
$[\alpha]^{20}_D$ = -228.6 (*c* = 0.14 acetone) (ee = 99%).

(*S*)-*N*-(2-(5-(4-(1-((4,6-diaminopyrimidin-2-yl)thio)ethyl)-5-methylthiazol-2-yl)-2-methoxyphenoxy)ethyl)methane-sulfonamide (12S = S-DI-82).
$[\alpha]^{19}_D$ = -536.4 (*c* = 0.11 acetone) (ee = 99%).

TOC Graphic

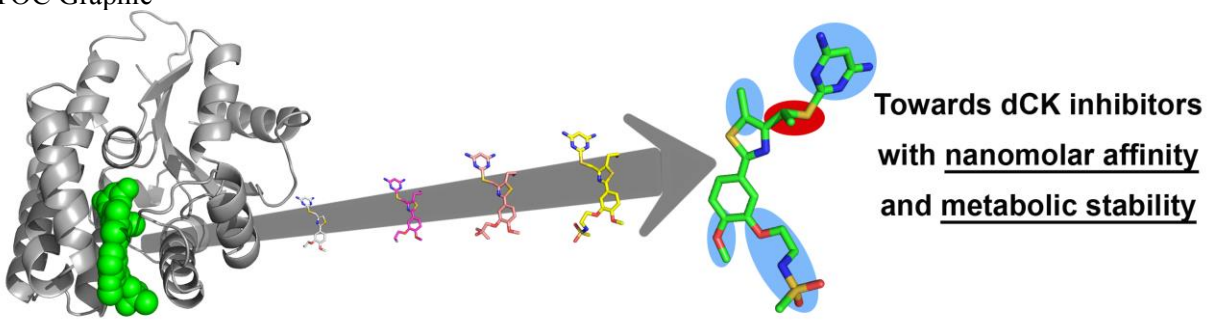
Towards dCK inhibitors
with nanomolar affinity
and metabolic stability